Available online at www.sciencedirect.com
ScienceDirect
Journal of Power Sources 166 (2007) 317–323
JOURNAL OF POWER SOURCES
www.elsevier.com/locate/jpowsour

Influence of different buffer solutions on the performance of anodic Pt-Ru/C nanoparticle electrocatalysts for a direct methanol fuel cell

Zhen-Bo Wang [a,*], Ge-Ping Yin [a], Peng-Fei Shi [a], Bo-Qian Yang [b], Peter-Xian Feng [b]

[a] *Department of Applied Chemistry, Harbin Institute of Technology, Harbin 150001, China*
[b] *Department of Physics, University of Puerto Rico, P.O. Box 23343, San Juan, PR 00931, USA*

Received 19 November 2006; received in revised form 18 December 2006; accepted 19 December 2006
Available online 12 February 2007

Abstract

This research aims to improve the activity of Pt-Ru nanoparticle electrocatalysts and thus, to lower the catalyst loading in anodes for methanol electrooxidation. The direct methanol fuel cell (DMFC) anodic Pt-Ru/C nanoparticle electrocatalysts were prepared using a chemical reduction method. The pH values of the reductive solutions were adjusted by different buffer solutions of CH_3COONa–NaOH, $C_6H_5Na_3O_7$–NaOH, and Na_2CO_3–$NaHCO_3$, respectively. The performance of the nanoparticle electrocatalysts were examined by cyclic voltammetry, chronoamperometry, and amperometric *i*–*t* curves using a glassy carbon working electrode in a solution of 0.5 mol L^{-1} CH_3OH and 0.5 mol L^{-1} H_2SO_4. The structures and micro-morphology of the Pt-Ru/C nanoparticles were determined and observed by X-ray diffraction (XRD) and transmission electron microscopy. XRD analysis showed that all of catalysts exhibited face-centered cubic (fcc) structures. No diffraction peaks indicated the presence of either pure Ru or Ru-rich hexagonal close packed (hcp) phase. The size of the Pt-Ru/C nanoparticles prepared with a $C_6H_5Na_3O_7$–NaOH solution was relatively small ~4.3 nm. Its size distribution in carbon was more homogeneous. The electrochemical active measurements results showed that the catalytic activity and the stability of Pt-Ru/C nanoparticle electrocatalyst prepared with a $C_6H_5Na_3O_7$–NaOH solution for methanol electrooxidation was higher than that from the other solutions due to the citrate complexation stabilizing effect and a competing adsorption effect.

Keywords: Direct methanol fuel cell; Methanol electrooxidation; Pt-Ru/C nanoparticle electrocatalyst; Different buffer solutions

1. Introduction

Hydrogen/air proton exchange membrane fuel cells (PEMFC) are receiving much interest for transportation applications because of the high power densities that they can generate at relatively low temperatures [1]. However, it is well known that hydrogen as a fuel presents several technological problems of production, storage, and transportation [2,3]. Because of this, methanol has been considered as the most promising organic fuel since it is more efficiently oxidized than other alcohols [4]. The past decades have viewed a significant effort to develop the direct methanol fuel cell (DMFC) which uses methanol directly without prior reforming [5–8]. Although a lot of progress has been made in the development of the DMFC, its performance is still limited by the poor kinetics of the anode reaction and the crossover of methanol from the anode to the cathode side through the polymer proton exchange membrane [9–11]. For high power applications, such as laptops, PDAs, and camcorders, it is necessary to enhance the cell performance further in order to compete with the lithium ion battery [12–14].

Ru is widely known as a second metal that promotes methanol electrooxidation. The promotion effect has been mainly discussed based on the so-called 'bifunctional mechanism' [15–21]. But, the activity of Pt-Ru alloy catalysts cannot satisfy the performance requirement of a DMFC, especially at low temperatures. There is a need to improve the activity of catalysts for methanol electrooxidation still further [22–24].

* Corresponding author. Present address: Department of Chemistry, University of Puerto Rico-Rio Piedras Campus, San Juan, PR 00931, USA.
Tel.: +1 787 7640000x7465; fax: +1 787 7641588.
E-mail address: wangzhenbo1008@yahoo.com.cn (Z.-B. Wang).

0378-7753/$ – see front matter © 2007 Elsevier B.V. All rights reserved.
doi:10.1016/j.jpowsour.2006.12.110

The performance, structure, dispersivity, and morphology of the catalysts are influenced by the preparation methods and different technics [25–27]. At present, Pt-Ru catalysts were often prepared by using the chemical reduction of H_2PtCl_6 and $RuCl_3$ as the precursors with HCHO as the reducing agent. But, HCOOH is formed in the preparative process, and the pH value of the reductive solution rapidly falls. This results in the reductive ratio of Pt and Ru compound precursors decreasing, the particle size of the catalyst increasing, and its catalytic activity for methanol electrooxidation decreasing [28]. Based on above literature findings, we think, it is meaningful to explore Pt-Ru/C catalysts prepared using a buffer solution to adjust the pH value of the reductive solution. Using this process we have investigated methanol electrooxidation on these electrocatalysts prepared with three different buffer solutions.

2. Experimental details

2.1. Preparation of catalysts

The Pt-Ru/C catalysts were prepared according to the method mentioned in literature [29–31]. Carbon black powder (Vulcan XC-72 with a specific BET area of 250 $m^2\,g^{-1}$ and average size of 40 nm, Cabot Corporation) was used as the support for the catalyst. The samples contained 20% metal by weight. The Pt-Ru (with an atomic ratio of 1:1)/C catalyst, 0.25 g, was obtained by chemical reduction with formaldehyde solution of H_2PtCl_6 and $RuCl_3$ as precursors at 80 °C. The carbon black was ultrasonically dispersed in a mixture of ultrapure water and isopropyl alcohol for 20 min. The Pt and Ru compounds precursors were added to the carbon ink and then mixed thoroughly for 15 min. The pH value of the ink was adjusted by CH_3COONa–NaOH, $C_6H_5Na_3O_7$–NaOH, or Na_2CO_3–$NaHCO_3$ solution to 8 and then raised its temperature to 80 °C. Ten millilitres of 1 mol L^{-1} solution of formaldehyde was added into the ink drop by drop and the bath was stirred for 1 h. The mixture was cooled, dried, and washed repeatedly with heated ultrapure water (MilliQ, Millipore, 18.2 MΩ cm) until no Cl^- ions existed. The catalyst powder was dried for 3 h at 120 °C and then stored in a vacuum vessel. All chemicals used were of analytical grade.

2.2. Preparation of working electrode and its electrochemical measurements

2.2.1. Preparation of working electrode

Glassy carbon working electrodes, 3 mm in diameter (electrode area 0.0706 cm^2), polished with 0.05 μm alumina to a mirror-finish before each experiment, were used as substrates for the carbon supported nanoparticle electrocatalysts. For the electrode preparation, 5 μL of an ultrasonically redispersed nanoparticle electrocatalysts suspension was pipetted onto the glassy carbon substrate. After the solvent evaporation, the deposited catalyst (28 $\mu g_{metal}\,cm^{-2}$) was covered with 5 μL of a dilute Nafion solution (5 wt.%). The resulting Nafion film with a thickness of ≤0.2 μm had a sufficient strength to attach the carbon supported Pt-Ru nanoparticles permanently to the glassy carbon electrode without producing significant film diffusion resistances [32,33].

2.2.2. Electrochemical measurements

Electrochemical measurements were carried out with a conventional three-electrode electrochemical cell at 25 °C. The glassy carbon thin film electrode as the working electrode (electrode area 0.0706 cm^2) was covered with the electrocatalyst powder. A piece of Pt foil of 1 cm^2 area was used as the counter electrode. The reversible hydrogen electrode (RHE) was used as the reference electrode with its solution connected to the working electrode by a Luggin capillary whose tip was placed close to the working electrode. All potential values reported are versus RHE. All chemicals used were of analytical grade. All the solutions were prepared with ultrapure water (MilliQ, Millipore, 18.2 MΩ cm). A solution of 0.5 mol L^{-1} CH_3OH and 0.5 mol L^{-1} H_2SO_4 was stirred constantly and purged with ultrapure argon gas. Electrochemical experiments were performed using a CHI630A electrochemical analysis instrument. Cyclic voltammograms (CV) were plotted within a potential range from 0.05 to 1.2 V with a scanning rate of 0.02 V s^{-1}. The chronoamperometric and amperometric *i–t* curves were carried out by using CHI630A electrochemical analysis instrument controlled by an IBM PC. The potential jumped from 0.1 to 0.8 V. Due to a slight contamination from the Nafion film, the thin film working electrodes were electrochemically cleaned by continuous cycling at 0.05 V s^{-1} until a stable response was obtained before the measurement curves were recorded.

2.3. Physical measurements

2.3.1. X-ray diffraction (XRD)

XRD patterns reveal the bulk structure of the catalyst and its support. XRD analysis was carried out for the nanoparticle electrocatalysts with a D/max-rB (Japan) diffractometer using a Cu Kα X-ray source operating at 45 kV and 100 mA. The XRD patterns were obtained at a scanning rate of 4° min^{-1} with an angular resolution of 0.05° of the 2θ scan.

2.3.2. Transmission electron micrographs (TEM)

TEM for the nanoparticle electrocatalysts samples were taken by a Japan JEOL JEM-1200EX transmission electron microscope with a spatial resolution of 1 nm. Before taking the electron micrographs, the nanoparticle samples were finely ground and ultrasonically dispersed in isopropyl alcohol, and a drop of the resultant dispersion was deposited and dried on a standard copper grid coated with a polymer film. The applied voltage was 100 kV with a magnification of 200,000 for the nanoparticles.

3. Results and discussion

3.1. Effect of buffer solution on structure of the nanoparticle electrocatalysts

Fig. 1 shows the XRD patterns of the nanoparticle electrocatalysts prepared with three different buffer solutions. The curves

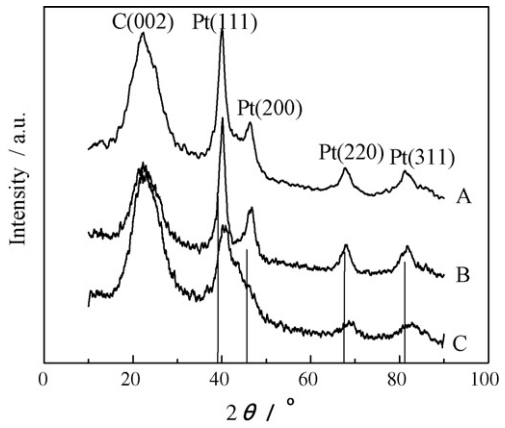

Fig. 1. XRD patterns of the Pt-Ru/C nanoparticles prepared with different buffer solutions: (A) CH_3COONa–NaOH, (B) $C_6H_5O_7Na_3$–NaOH, and (C) Na_2CO_3–$NaHCO_3$.

A–C in Fig. 1 are XRD patterns of nanoparticles which were prepared with CH_3COONa–NaOH, $C_6H_5Na_3O_7$–NaOH, and Na_2CO_3–$NaHCO_3$ solutions, respectively. It can be seen that the first peak in the XRD pattern is associated with the carbon support. The other four peaks are characteristic of face-centered cubic (fcc) crystalline Pt, corresponding to the planes (1 1 1), (2 0 0), (2 2 0), and (3 1 1) at 2θ values of ca. 39.8, 46.5, 67.8, and 81.2°, respectively, indicating that the alloy nanoparticles are principally single-phase disordered structures. But, the Pt (2 0 0) plane of the nanoparticles with Na_2CO_3–$NaHCO_3$ solution is indistinguishable as shown by curve C in Fig. 1, which indicates that the nanoparticles do not form a good crystal state. It is important to note that no diffraction peaks indicate the presence of either pure Ru, or Ru-rich hexagonal close packed (hcp) phase, which suggests that Ru atoms either form an alloy with Pt or exist as oxide in amorphous phases. Relative to the same reflections in bulk Pt (cf. the reference vertical lines of Pt in Fig. 1); the diffraction peaks for Pt-Ru alloy nanoparticles are slightly shifted to higher 2θ values. The higher angle shifts of the Pt diffraction peaks reveal the formation of an alloy involving the incorporation of Ru atom into the fcc structure of Pt.

The Pt (2 2 0) peak was selected to calculate the average particle size of Pt-Ru/C nanoparticles according to Debye–Scherrer formula [34,35] because it is isolated from the diffraction peaks carbon supports. The average particle sizes of Pt-Ru/C nanoparticle electrocatalysts prepared with CH_3COONa–NaOH, $C_6H_5Na_3O_7$–NaOH, and Na_2CO_3–$NaHCO_3$ solutions are 4.2, 4.3, and 3.3 nm, respectively. They are smaller than that with NaOH solution [28].

3.2. Effect of buffer solution on dispersion of the nanoparticle electrocatalysts

Fig. 2 shows the TEM images of Pt-Ru/C nanoparticles prepared with different buffer solutions. Fig. 2A–C are TEM images of nanoparticles prepared with CH_3COONa–NaOH, $C_6H_5Na_3O_7$–NaOH, and Na_2CO_3–$NaHCO_3$ solutions, respectively. The dark black portions are Pt-Ru grains, and the grey

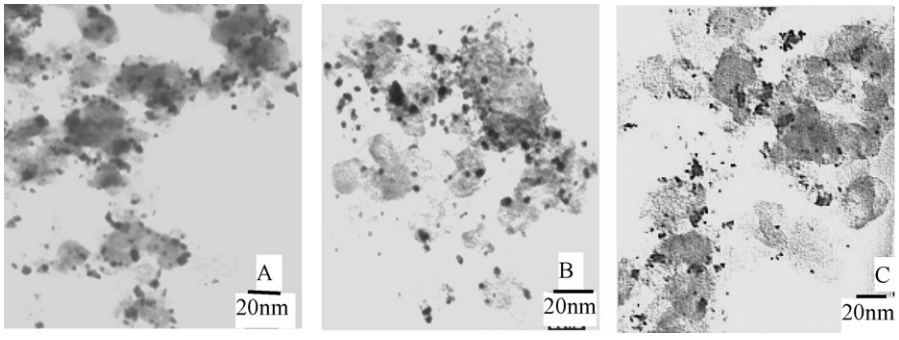

Fig. 2. TEM micrographs of the Pt-Ru/C nanoparticles prepared with different buffer solutions: (A) CH_3COONa–NaOH, (B) $C_6H_5O_7Na_3$–NaOH, and (C) Na_2CO_3–$NaHCO_3$.

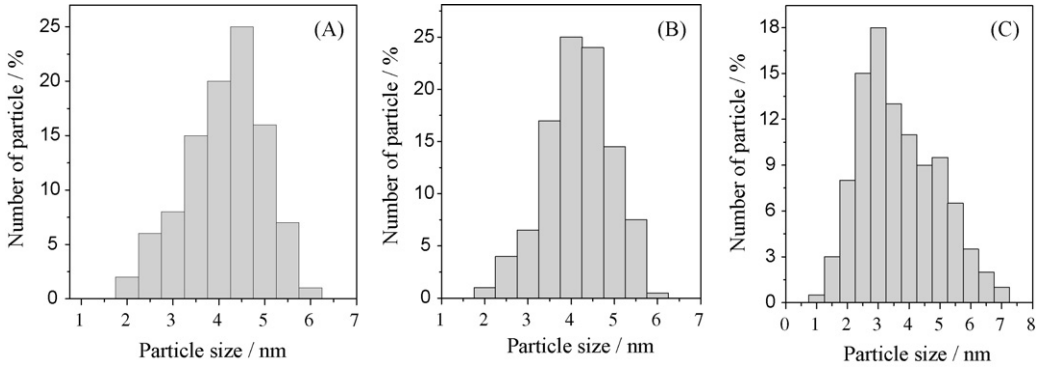

Fig. 3. Size distribution of the Pt-Ru particles of the Pt-Ru/C nanoparticle electrocatalysts prepared with different buffer solutions: (A) CH_3COONa–NaOH, (B) $C_6H_5O_7Na_3$–NaOH, and (C) Na_2CO_3–$NaHCO_3$.

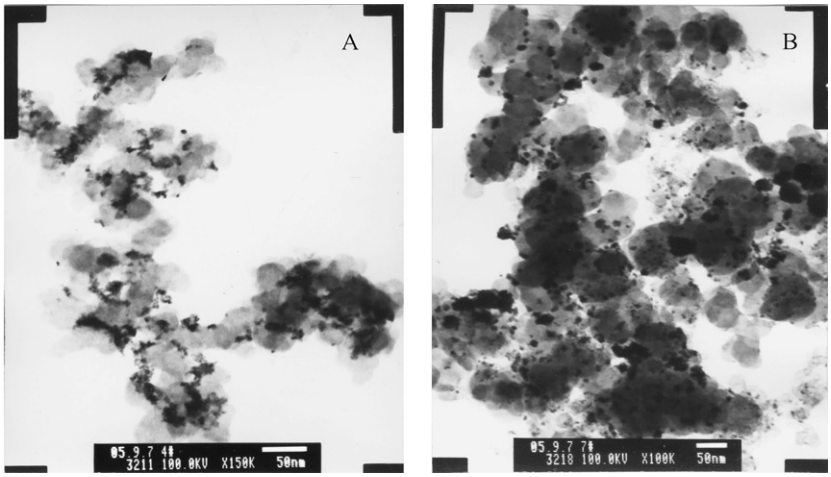

Fig. 4. TEM micrographs of the Pt-Ru/C nanoparticles prepared with different buffer solutions: (A) CH_3COONa–NaOH and (B) $C_6H_5O_7Na_3$–NaOH.

portions are carbon support grains. It can be seen that the dispersion of the nanoparticles prepared with CH_3COONa–NaOH and $C_6H_5Na_3O_7$–NaOH solutions are homogeneous and without agglomeration. The particle sizes of the Pt-Ru/C nanoparticles are small. The dispersion of the nanoparticles with Na_2CO_3–$NaHCO_3$ solution is uneven with a certain extent of agglomeration.

Fig. 3 presents the size distribution of Pt-Ru particles of Pt-Ru/C nanoparticle electrocatalysts prepared with different buffer solutions. Fig. 3A–C shows the size distributions of the nanoparticles prepared with CH_3COONa–NaOH, $C_6H_5Na_3O_7$–NaOH, and Na_2CO_3–$NaHCO_3$ solutions, respectively.

The values of Pt-Ru particle mean diameter are the number averaged diameters of the Pt-Ru nanoparticles in samples, which can be calculated from TEM measurements of individual particle diameters, d_i, using the following equation [36]:

$$\bar{d}_n = \frac{\sum_{i=1}^{n} d_i}{n} \quad (1)$$

where $\bar{d}_n$ is the number averaged diameter of Pt-Ru particles in nanometer. The averaged particle sizes of Pt-Ru/C nanoparticles prepared with CH_3COONa–NaOH, $C_6H_5Na_3O_7$–NaOH, and Na_2CO_3–$NaHCO_3$ solutions are 4.5, 4.6, and 3.7 nm, respectively. It is consistent with the particle sizes calculated from XRD patterns. Fig. 3 shows that the range of size distribution of Pt-Ru/C nanoparticles prepared with CH_3COONa–NaOH and $C_6H_5Na_3O_7$–NaOH solutions are relatively narrow, whereas, its of nanoparticles prepared with Na_2CO_3–$NaHCO_3$ solution is relatively wide.

Fig. 4 shows the representative TEM images of Pt-Ru/C nanoparticles prepared with CH_3COONa–NaOH and $C_6H_5Na_3O_7$–NaOH after electrochemical measurements. It can be seen from the TEM images that the size of Pt-Ru nanoparticles increases after long time measurements in both cases. The Pt-Ru particle size distributions obtained from image analysis are shown in the histograms in Fig. 5. Comparing with the original ones (Fig. 3), the Pt-Ru particle sizes distribution are enlarged for the catalysts after long time. The number of Pt-Ru particles with small diameters (2.0 nm) largely decreases or disappears, and larger Pt-Ru particles (larger than 6 nm) appear. It can be believed that the small Pt particles were "swallowed up" by the larger ones through the migration of small Pt-Ru particles on the carbon surface [37,38] or through the Pt ions (e.g., Pt^{2+}) dissolution/redeposition process [39,40]. The mean sizes (diameter) of

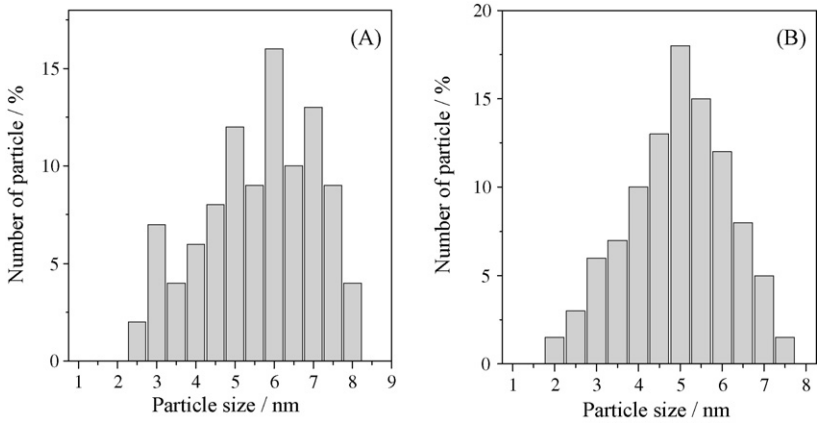

Fig. 5. Size distribution of the Pt-Ru particles of the Pt-Ru/C nanoparticle electrocatalysts prepared with different buffer solutions: (A) CH_3COONa–NaOH and (B) $C_6H_5O_7Na_3$–NaOH.

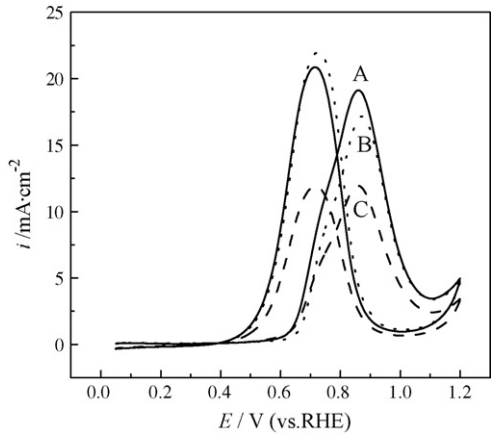

Fig. 6. Cyclic voltammograms of methanol electrooxidation in a solution of 0.5 mol L^{-1} CH_3OH and 0.5 mol L^{-1} H_2SO_4 at 25 °C on the Pt-Ru/C nanoparticle electrocatalysts prepared with different buffer solutions: (A) CH_3COONa–NaOH, (B) $C_6H_5O_7Na_3$–NaOH, and (C) Na_2CO_3–$NaHCO_3$. Scan rate: 0.02 V s^{-1}.

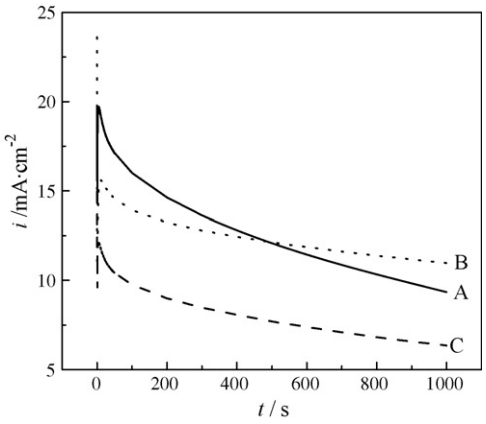

Fig. 7. Chronoamperometric curves of methanol electrooxidation in a solution of 0.5 mol L^{-1} CH_3OH and 0.5 mol L^{-1} H_2SO_4 at 25 °C on the Pt-Ru/C nanoparticle electrocatalysts prepared with different buffer solutions: (A) CH_3COONa–NaOH, (B) $C_6H_5O_7Na_3$–NaOH, and (C) Na_2CO_3–$NaHCO_3$. Potential jumps from 0.1 to 0.8 V.

the Pt-Ru/C nanoparticles prepared with CH_3COONa–NaOH and $C_6H_5Na_3O_7$–NaOH solutions after electrochemical measurements are 5.8 and 5.0 nm, respectively.

3.3. Effect of buffer solution on catalytic activity of the nanoparticle electrocatalysts

Fig. 6 presents the cyclic voltammograms on the Pt-Ru/C nanoparticles prepared with different buffer solutions in a solution of 0.5 mol L^{-1} CH_3OH and 0.5 mol L^{-1} H_2SO_4 at 25 °C. The curves A–C in Fig. 6 are CV curves of nanoparticles prepared with CH_3COONa–NaOH, $C_6H_5Na_3O_7$–NaOH, and Na_2CO_3–$NaHCO_3$ solutions, respectively.

It can be seen from Fig. 6 that the onset potential of a current rise for methanol electrooxidation on the three Pt-Ru/C nanoparticles are almost the same, i.e., about 0.55 V. The peak potential for methanol electrooxidation, at which the peak current occurs is 0.86 V (versus RHE), and the peak current density is 19.1 mA cm^{-2} during positive potential scanning on the Pt-Ru/C nanoparticles prepared with CH_3COONa–NaOH solution as shown by curve A. The peak potential for methanol electrooxidation and the peak current density on the Pt-Ru/C nanoparticles prepared with $C_6H_5Na_3O_7$–NaOH solution are about 0.87 V (versus RHE) and 17.2 mA cm^{-2}, respectively, during positive potential scanning as shown by curve B. The peak potential for methanol electrooxidation and the peak current density on the Pt-Ru/C nanoparticles prepared with Na_2CO_3–$NaHCO_3$ solution are about 0.86 V (versus RHE) and 11.9 mA cm^{-2}, respectively, during positive potential scanning as shown by curve C. The peak potential on the Pt-Ru/C nanoparticles with CH_3COONa–NaOH and Na_2CO_3–$NaHCO_3$ solutions during potential scanning is 10 mV lower than that with $C_6H_5Na_3O_7$–NaOH solution. But, the peak current density on the Pt-Ru/C nanoparticles with CH_3COONa–NaOH solution is only 1.9 mA cm^{-2} higher than that with $C_6H_5Na_3O_7$–NaOH solution. The peak current density on the Pt-Ru/C nanoparticles with Na_2CO_3–$NaHCO_3$ solution is the smallest.

The catalytic activities of the nanoparticle electrocatalysts for methanol electrooxidation measured as steady-state current densities at a constant potential were used to compare the performance of the electrocatalysts. Fig. 7 shows the current densities measured at a constant potential jumping from 0.1 to 0.8 V in an Ar-saturated solution of 0.5 mol L^{-1} CH_3OH and 0.5 mol L^{-1} H_2SO_4 at 25 °C. Initial high current mainly correspond to double layer charging. The currents decay with time in a parabolic style, and reach an apparent steady-state within 500 s. The current density of methanol electrooxidation on the Pt-Ru/C nanoparticles prepared with $C_6H_5O_7Na_3$–NaOH solution, which is a 11.0 mA cm^{-2} at 1000 s as shown by curve B, is almost the twice as high as that on the Pt-Ru/C nanoparticles with Na_2CO_3–$NaHCO_3$ solution by curve C at the same potential and the same time, is evidently higher than that on the Pt-Ru/C nanoparticles with CH_3COONa–NaOH solution by curve A. It can be seen that the catalytic activity of Pt-Ru/C nanoparticles with CH_3COONa–NaOH solution for methanol electrooxidation is higher than that with $C_6H_5O_7Na_3$–NaOH solution during initial reaction stages (within 500 s). But with running time, the current density of the nanoparticles with CH_3COONa–NaOH solution is rapidly decreasing. Its current density is lower than that with $C_6H_5O_7Na_3$–NaOH solution at 500 s later. The catalytic activity of Pt-Ru/C nanoparticles with Na_2CO_3–$NaHCO_3$ solution for methanol electrooxidation is the lowest during the whole running time. The results are a little different from those of cyclic voltammetry measurement.

3.4. Effect of buffer solution on stability of the nanoparticle electrocatalysts

Fig. 8 shows the Amperometric current–time (*i*–*t*) curves measured at a constant potential 0.8 V on the Pt-Ru/C nanoparticle electrocatalysts prepared with different buffer solutions in a solution of 0.5 mol L^{-1} CH_3OH and 0.5 mol L^{-1} H_2SO_4 at 25 °C. The curves A–C in Fig. 8 are the *i*–*t* curves of the nanoparticle electrocatalysts prepared with CH_3COONa–NaOH,

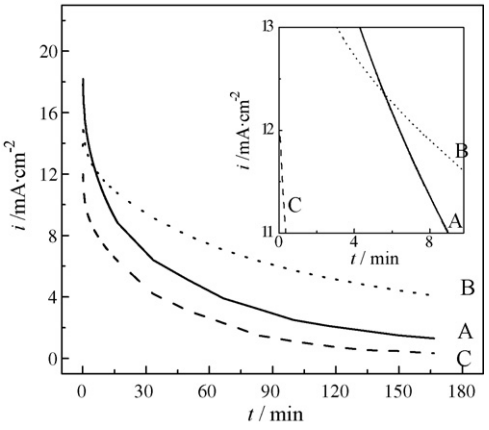

Fig. 8. Amperometric *i–t* curves of methanol electrooxidation in a solution of 0.5 mol L^{-1} CH_3OH and 0.5 mol L^{-1} H_2SO_4 at 25 °C on the Pt-Ru/C nanoparticle electrocatalysts prepared with different buffer solutions: (A) CH_3COONa–NaOH, (B) $C_6H_5O_7Na_3$–NaOH, and (C) Na_2CO_3–$NaHCO_3$. Potential is 0.8 V.

$C_6H_5Na_3O_7$–NaOH, and Na_2CO_3–$NaHCO_3$ solutions, respectively. The current density of methanol electrooxidation on the Pt-Ru/C nanoparticles prepared with $C_6H_5O_7Na_3$–NaOH solution is the highest, which is 4.8 mA cm^{-2} at 10,000 s as shown by curve B, i.e., its catalytic activity and stability is the best. The stability for methanol electrooxidation on the nanoparticles with CH_3COONa–NaOH solution is relatively bad. Its current density is very small, which is 1.3 mA cm^{-2} at 10,000 s by curve A. However, the current density of curve A is higher than that of curve B during the initial running stage (400 s ago). The decreasing rate of current density of curve A is faster than that of curve B during the running time (the amplified parts of curves as shown in Fig. 8). The stability of the nanoparticles with Na_2CO_3–$NaHCO_3$ solution is the lowest. Its current density is smallest, which is a 0.32 mA cm^{-2} at 10,000 s. The results are similar to those of chronoamperometric curve measurements.

Following reaction equations that formaldehyde reduces H_2PtCl_6 and $RuCl_3$ as precursors, the medium reactions should happen in alkaline medium [28,29].

$$H_2PtCl_6 + 2NaOH \rightarrow Na_2PtCl_6 + 2H_2O \quad (2)$$

$$Na_2PtCl_6 + 4NaOH + 2HCHO \rightarrow 2HCOOH + Pt + 6NaCl + 2H_2O \quad (3)$$

$$Na_2PtCl_6 + 4NaOH + 2HCOOH \rightarrow 2CO_2 + Pt + 6NaCl + 4H_2O \quad (4)$$

Overall reaction:

$$H_2PtCl_6 + HCHO + 6NaOH \rightarrow CO_2 + Pt + 6NaCl + 5H_2O \quad (5)$$

$$RuCl_3 + 3NaOH \rightarrow Ru(OH)_3 \downarrow + 3NaCl \quad (6)$$

$$2Ru(OH)_3 + 3HCHO \rightarrow 2Ru + 3HCOOH + 3H_2O \quad (7)$$

$$2Ru(OH)_3 + 3HCOOH \rightarrow 2Ru + 3CO_2 + 6H_2O \quad (8)$$

Overall reaction:

$$4RuCl_3 + 12NaOH + 3HCHO \rightarrow 4Ru + 3CO_2 + 9H_2O + 12NaCl \quad (9)$$

It can be seen from Eq. (4) and (7) that HCOOH is formed during the reductive reaction process, meanwhile the pH value of reductive solution is decreasing rapidly. The effect of the buffer solution directly relates to the chemical equilibrium of buffer solution. If the buffer solution is used to adjust the pH value of reductive solution, the chemical equilibrium can be kept because the buffer solution can ionize enough OH^- ions. The H^+ ions from HCOOH ionization are neutralized by OH^- ions which are provided by the buffer solution during reductive reaction. Due to sufficient OH^- ions being provided, the pH value of the reductive solution changes little [28]. The reductive ratio of Pt and Ru compounds precursors are relatively fast. The formation rate of the Pt and Ru nuclei is higher. The particle sizes of the nanoparticle electrocatalysts decrease and their active surface specific areas increase, i.e., their catalytic activity for methanol electrooxidation enhance.

It is usually considered that the $PtCl_6^{2-}$ ions are firstly reduced to $PtCl_4^{2-}$ ions by surface active sites on carbon support when the Pt and Ru compounds precursors are adsorbed [41]. The latter is reversibly adsorbed on the carbon support surface and can shift through diffusion. Pt nuclei grow when the $PtCl_4^{2-}$ ions meet the reduced Pt crystalline nucleus. The $PtCl_4^{2-}$ ions have two species of strongly and weakly adsorptions due to the surface functional group of carbon. The diffusion rate of the weakly adsorption $PtCl_4^{2-}$ ions is relatively rapid on the carbon surface. They favor crystalline particle growth, rather than forming new crystalline nuclei. But, it is just the opposite when the diffusion rate of the strongly adsorption $PtCl_4^{2-}$ ions is relatively slow and favors forming new Pt crystalline nucleus, which yields small size and highly dispersed Pt-Ru nanoparticles [41]. The Na_2CO_3–$NaHCO_3$ solution can only ionize OH^- ions which keep the pH value of reductive solution in this paper, so the performance of the Pt-Ru/C nanoparticles prepared with it is relatively bad. The CH_3COONa–NaOH and $C_6H_5O_7Na_3$–NaOH solutions, not only keep the pH value of reductive solution, but also play an important role in which the CH_3COO^- and $C_6H_5O_7^-$ ions can compete with the $PtCl_4^{2-}$ ions for the active sites on the carbon support surface, which can decrease or eliminate the number of the weakly adsorbed $PtCl_4^{2-}$, and then the strongly adsorbed $PtCl_4^{2-}$ ions dominate the carbon support surface. So, the particle sizes of the Pt-Ru/C nanoparticles are relatively small, and their distribution on carbon surface are very even. On the other hand, the radius of the CH_3COO^- ion is different from that of the $C_6H_5O_7^-$ ion. The competition between CH_3COO^-/$C_6H_5O_7^-$ ions and the $PtCl_4^{2-}$ ions results in a different distance between the $PtCl_4^{2-}$ ions, i.e., the distance of the reduced Pt-Ru nanoparticles on the carbon surface is different. The distance of the Pt-Ru nanoparticle electrocatalyst prepared with the $C_6H_5O_7Na_3$–NaOH solution is relatively farther than

that with CH_3COONa–NaOH solution because the radius of the $C_6H_5O_7^-$ ion is bigger than that of CH_3COO^- ion. The distribution of the nanoparticles with the former is more even than that of the latter. The growth rate of the Pt-Ru nanoparticles prepared with a $C_6H_5O_7Na_3$–NaOH solution is slow i.e., its stability is relatively better (see Figs. 4 and 5). On the contrary, the catalytic activity of the electrocatalyst with CH_3COONa–NaOH solution is high during the initial run time, but, the growth rate of the Pt-Ru nanoparticles is relatively fast, so its activity for methanol electrooxidation decreases markedly with time, i.e., its stability is bad. In addition, the $C_6H_5O_7^-$ ions also play a role in stabilizing the Pt-Ru metal nanoparticles [42,43], which is another reason why the stability of the Pt-Ru nanoparticles is better.

4. Conclusions

The Pt-Ru/C nanoparticle electrocatalysts prepared with different buffer solutions were investigated for their methanol electrooxidation. The distribution of the nanoparticle electrocatalysts with $C_6H_5O_7Na_3$–NaOH solution was very homogeneous, the distance of the Pt-Ru nanoparticles from each other on the carbon surface was relatively far, due to the citrate complexation stabilizing effect and the competing adsorption effects, its catalytic activity for methanol electrooxidation was the highest, and its stability was the best during a lifetime measurement. Although the distribution of the nanoparticle electrocatalyst with a CH_3COONa–NaOH solution was very even, its catalytic activity for methanol electrooxidation was higher, the distance of the Pt-Ru nanoparticles between each other was relatively small, and the Pt-Ru particles size rapidly grew during lifetime measurement, and so its stability markedly decreased. The catalytic activity and the stability of the electrocatalyst using a Na_2CO_3–$NaHCO_3$ solution were the lowest for methanol electrooxidation.

Acknowledgements

This work is supported financially by the National Natural Science Foundation of China (Grant No. 20606007) and Heilongjiang Natural Science Foundation (B0201).

References

[1] N. Wagner, M. Schulze, Electrochim. Acta 48 (2003) 3899.
[2] Y.-J. Leng, X. Wang, I.-M. Hsing, J. Electroanal. Chem. 528 (2002) 145.
[3] S.J.C. Cleghorn, T.E. Springer, M.S. Wilson, C. Zawodzinski, T.A. Zawodzinski, S. Gottesfeld, Int. J. Hydrogen Energy 22 (1997) 1137.
[4] A.O. Neto, T.R.R. Vasconcelos, R.W.R.V. Da Silva, M. Linardi, E.V. Spinac, J. Appl. Electrochem. 35 (2005) 193.
[5] A.O. Neto, M.J. Giz, J. Perez, E.A. Ticianelli, E.R. Gonzalez, J. Electrochem. Soc. 149 (2002) A272.
[6] A.K. Shukla, M.K. Ravikumar, M. Neergat, K.S. Gandhi, J. Appl. Electrochem. 29 (1999) 129.
[7] H. Dohle, H. Schmitz, T. Bewer, J. Mergel, D. Stolten, J. Power Sources 106 (2002) 313.
[8] H. Dohle, J. Divisek, J. Mergel, H.F. Oetjen, C. Zingler, D. Stolten, J. Power Sources 105 (2002) 274.
[9] W. Sugimoto, K. Aoyama, T. Kawaguchi, Y. Murakami, Y. Takasu, J. Electroanal. Chem. 576 (2005) 215.
[10] S.C. Thomas, X.M. Ren, S. Gottesfeld, P. Zelenay, Electrochim. Acta 47 (2002) 3741.
[11] E. Antolini, J.R.C. Salgado, E.R. Gonzalez, J. Electroanal. Chem. 580 (2005) 145.
[12] Z.B. Wang, G.P. Yin, J. Zhang, Y.C. Sun, P.F. Shi, Electrochim. Acta 51 (2006) 5691.
[13] G.Q. Lu, C.Y. Wang, J. Power Sources 144 (2005) 141.
[14] K.W. Park, B.K. Kwon, J.H. Choi, I.S. Park, Y.M. Kim, Y.E. Sung, J. Power Sources 109 (2002) 439.
[15] T. Page, R. Johnson, J. Hormes, S. Noding, B. Rambabu, J. Electroanal. Chem. 485 (2000) 34.
[16] S. Mukerjee, R.C. Urian, Electrochim. Acta 47 (2002) 3219.
[17] L. Giorgi, A. Pozio, C. Bracchini, R. Giorgi, S. Turtu, J. Appl. Electrochem. 31 (2001) 325.
[18] A. Pozio, M. de Francesco, A. Cemmi, F. Cardellini, L. Giorgi, J. Power Sources 105 (2002) 13.
[19] C.L. Green, A. Kucernak, J. Phys. Chem. B 106 (2002) 1036.
[20] S.A. Kirillov, P.E. Tsiakaras, I.V. Romanova, J. Mol. Struct. 651–653 (2003) 365.
[21] A.V. Tripkovic, K.Dj. Popovic, J.D. Lovic, Electrochim. Acta 46 (2001) 3163.
[22] F.J. Rodriguez-Nieto, T.Y. Morante-Catacora, C.R. Cabrera, J. Electroanal. Chem. 571 (2004) 15.
[23] J.S. Guo, G.Q. Sun, Q. Wang, G.X. Wang, Z.H. Zhou, S.H. Tang, L.H. Jiang, B. Zhou, Q. Xin, Carbon 44 (2006) 152.
[24] Y.M. Liang, H.M. Zhang, B.L. Yi, Z.H. Zhang, Z.C. Tan, Carbon 43 (2005) 3144.
[25] W.C. Choi, J.D. Kim, S.I. Woo, Catal. Today 74 (2002) 235.
[26] X. Wang, I.M. Hsing, Electrochim. Acta 47 (2002) 2981.
[27] C.H. Lee, C.W. Lee, D.I. Kim, D.H. Jung, C.S. Kim, D.R. Shim, J. Power Sources 86 (2000) 478.
[28] Z.B. Wang, G.P. Yin, P.F. Shi, Chin. J. Catal. 26 (2005) 923.
[29] Z.B. Wang, G.P. Yin, P.F. Shi, Carbon 44 (2006) 133.
[30] Z.B. Wang, G.P. Yin, P.F. Shi, J. Harbin Inst. Technol. 38 (2006) 724.
[31] Z.B. Wang, G.P. Yin, P.F. Shi, J. Harbin Inst.Technol. 38 (2006) 541.
[32] T.J. Schmidt, H.A. Gasteiger, G.D. Stab, P.M. Urban, D.M. Kolb, R.J. Behm, J. Electrochem. Soc. 145 (1998) 2354.
[33] Z.B. Wang, G.P. Yin, P.F. Shi, Acta Phys.-Chim. Sinica 21 (2005) 1156.
[34] C.Z. He, H.R. Kunz, J.M. Fenton, J. Electrochem. Soc. 144 (1997) 970.
[35] Z.B. Wang, G.P. Yin, P.F. Shi, J. Electrochem. Soc. 152 (2005) A2406.
[36] P.J. Ferreira, G.J. la O, Y. Shao-Horn, D. Morgan, R. Makharia, S. Kocha, H.A. Gasteiger, J. Electrochem. Soc. 152 (2005) A2256.
[37] H.R. Colon-Mercado, H. Kim, B.N. Popov, Electrochem. Commun. 6 (2004) 795.
[38] Y.Y. Shao, G.P. Yin, Y.Z. Gao, P.F. Shi, J. Electrochem. Soc. 153 (2006) A1093.
[39] M.S. Wilson, F.H. Garzon, K.E. Sickafus, S. Gottesfeld, J. Electrochem. Soc. 140 (1993) 2872.
[40] R.M. Darling, J.P. Meyers, J. Electrochem. Soc. 150 (2003) A1523.
[41] H.E. Vandam, H.V. Bekkum, J. Catal. 131 (1991) 335.
[42] Y.Q. Xu, X.F. Xie, J.W. Guo, S.B. Wang, Y.W. Wang, V.K. Mathur, J. Power Sources 162 (2006) 132.
[43] J.W. Guo, T.S. Zhao, J. Prabhuram, C.W. Wong, Electrochim. Acta 50 (2005) 1973.